Vol. 639: 53–71, 2020
https://doi.org/10.3354/meps13267

MARINE ECOLOGY PROGRESS SERIES
Mar Ecol Prog Ser

Published April 2

Planktonic primary production in the western Dutch Wadden Sea

P. Jacobs[1,*], J. C. Kromkamp[2], S. M. van Leeuwen[1], C. J. M. Philippart[1,3]

[1]NIOZ Royal Netherlands Institute for Sea Research, Department of Coastal Systems, and Utrecht University, PO Box 59, 1790 AB Den Burg, Texel, the Netherlands

[2]NIOZ Royal Netherlands Institute for Sea Research, Department of Estuarine and Delta Systems, and Utrecht University, PO Box 140, 4400 AC Yerseke, the Netherlands

[3]University of Utrecht, Department of Physical Geography, PO Box 80.115, 3508 TC Utrecht, the Netherlands

ABSTRACT: Pelagic primary production measurements provide fundamental information about the trophic status of a marine ecosystem. Measured carbon fixation rates generally have a limited temporal and spatial resolution, but can be combined with Earth Observation data to extrapolate the measurements. Here, *P–E* curves were fitted for 3 yr of ^{14}C incubation data from the western Wadden Sea, using 4 different models; 2 with and 2 without photo-inhibition. The curve-fit model by Jassby & Platt (1976) best fit the data. Applying this model showed that the photosynthetic parameters, normalised for chlorophyll *a* concentration, of maximum production (P^B_{max}) and initial slope of the *P–E* curve (α^B) were correlated. Seasonality in photosynthetic parameters of this model and the relationship with environmental variables were explored, with a focus on variables that can be inferred from satellite algorithms. There were no significant correlations between α^B and any of the environmental variables measured. While P^B_{max} correlated with sea surface temperature (SST), the vertical light attenuation coefficient, silicate and nitrate + nitrite concentration, the multivariate model that best explained the variation in estimates of P^B_{max} was a model that included SST and year. In the period from 2012–2014, daily and annual production ranged between 3.4 and 3800 mg C d^{-1} and between 131 and 239 g C m^{-2} yr^{-1}, respectively. Comparison of these results with historical data (1990–2003) indicates that the decline in planktonic primary production that has been happening since the 1990s has halted. Although not tested, we believe that our approach is generally applicable to coastal waters.

KEY WORDS: Production–light curve · Photosynthetic parameters · Environmental variables · ^{14}C incubations · Phytoplankton

1. INTRODUCTION

Measurements of planktonic primary production provide fundamental information about the trophic status of marine ecosystems (Pereira et al. 2013, Muller-Karger et al. 2018). Historically, measured carbon fixation rates have come from ^{14}C incubations (Longhurst et al. 1995). Not only are such measurements logistically difficult and expensive to sustain as part of long-term monitoring programs, these discrete measurements provide information that is valid at only a very small spatial and temporal scale (Behrenfeld & Falkowski 1997). Upscaling these measurements requires knowledge of the regional and seasonal distribution of algal biomass (Longhurst et al. 1995). Since 1978, this information has been available from satellite-retrieved data (Longhurst et al. 1995, Behrenfeld & Falkowski 1997). Although progress has been made since then, such remotely sensed data is far from perfect, with poor performance due to cloud cover and, in coastal areas, interference of suspended matter and coloured dissolved organic material (CDOM) concentrations with satellite signals, hampering a reliable estimate of the chlorophyll *a* (chl *a*)

*Corresponding author: pascalle.jacobs@nioz.nl

concentration (Joint & Groom 2000, Jamet et al. 2011, Aurin & Dierssen 2012, Chen et al. 2013). On the positive side, these shortcomings are partly compensated for by the large number of observations. Satellite-derived data can be combined with principles of algal physiology to potentially estimate primary production (Longhurst et al. 1995, Bouman et al. 2018).

Light availability is a critical factor controlling primary production (Cole & Cloern 1984, 1987, Pennock & Sharp 1994, Heip et al. 1995, Cloern 1999). Estimation of annual production from relatively few images per year is based on several assumptions, amongst others with respect to the relationship between productivity/carbon fixation rate (*P*) and light conditions (*E*). Annual productivity is generally calculated as the sum of daily productivity for all days of the year. Daily productivity can be derived from incubations of water samples with ^{14}C during a fixed period (often 1–2 h), i.e. *P*, at a range of *E* and the light conditions in the water column during the day. These daily light conditions in the water column are determined by the daily insolation at the water surface and light attenuation in the water column.

The resulting *P*–*E* curves have either 2 (in the absence of photo-inhibition) or 3 parameters (allowing photo-inhibition) and the rates are often normalised to the chl *a* concentration, giving the following parameters: α^B, P^B_{max} and, in case the model includes photo-inhibition, β^B. If photo-inhibition occurs, then applying a model without photo-inhibition is expected to overestimate water-column production (Platt et al. 1980). The actual occurrence of photo-inhibition, however, might also be exaggerated because of incubations that occur for too long at high light intensities, but the importance of this incubation artefact is hard to quantify (Peterson 1980, Grobbelaar 1985).

So far, satellite images have been able to supply data on light conditions, light attenuation in the water, chl *a* concentrations, sea surface temperatures (SSTs) and (more recently) salinity (Gabarró et al. 2004, Klemas 2011), but not on the details of the photosynthetic parameters α^B, P^B_{max} and β^B. If these parameters could be derived as well, this more complete data set would allow for more extensive monitoring of temporal and spatial variation such as shifts in the timing of phytoplankton blooms, gradients in pelagic production in river outflows and trends in overall productivity (Pereira et al. 2013). Modelling photosynthetic parameters as a function of temperature (Behrenfeld & Falkowski 1997, Cox et al. 2010) or of temperature and nutrients (Cox et al. 2010) would allow for indirect estimates of pelagic production from satellite data.

In this paper, *P*–*E* parameters derived from 2 h incubations in a photosynthetron were used to estimate daily and annual productivity. Four different models were applied, and the effect of model choice on the estimated productivity was compared. Using the best model for the data set, seasonality in the photosynthetic parameters and the relationships between the values of these parameters with environmental conditions (daily insolation, SST, salinity, turbidity, concentrations of nutrients and chl *a*) were explored. This analysis was based upon 3 yr (2012–2014) of ^{14}C incubation data derived from the Marsdiep, the westernmost tidal inlet of the Wadden Sea, a shallow subsystem separated from the North Sea (northern Europe) by a chain of barrier islands. This area was subjected to eutrophication in the mid-1970s, followed by a reduction in nutrient supply since the late 1980s (Philippart et al. 2000). These changes in trophic states were reflected in changes in biomass, species composition and production of phytoplankton (Philippart et al. 2000, 2007). Annual production rates during 2012–2014 were compared with data from 1990–2003 (Philippart et al. 2007) to explore whether the previously described decline has persisted.

2. MATERIALS AND METHODS

2.1. Data collection

Water samples were collected at high tide from the Royal Netherlands Institute for Sea Research (NIOZ) jetty (53° 00′ 06″ N, 4° 47′ 21″ E) in the Marsdiep tidal basin (Fig. 1). Depth at the sampling location was 3 m; the average depth in the Marsdiep tidal basin is 4.6 m (Ridderinkhof 1988, Cadée & Hegeman 2002). The samples were taken with a bucket, 40 times yr^{-1} with an average frequency of once wk^{-1} from March–September and approximately twice mo^{-1} from October–February. Water temperature (SST; °C) was measured directly using a bucket thermometer (unknown brand and type, accuracy 0.1°C); salinity (PSU) was measured by reading the refraction index of 0.2 µm filtered seawater that was acclimated to laboratory temperature, using a handheld refractometer (ENDECO type 102, accuracy 0.1‰). The refraction index (or salinity) was then corrected for temperature using temperature–salinity charts. Chl *a* concentrations were determined by filtering 250–500 ml water over Whatman GF/F filters (47 mm diameter); filters were quick-frozen in liquid nitrogen and subsequently stored at –80°C until analysis. Samples were analysed within 1 yr by high-perfor-

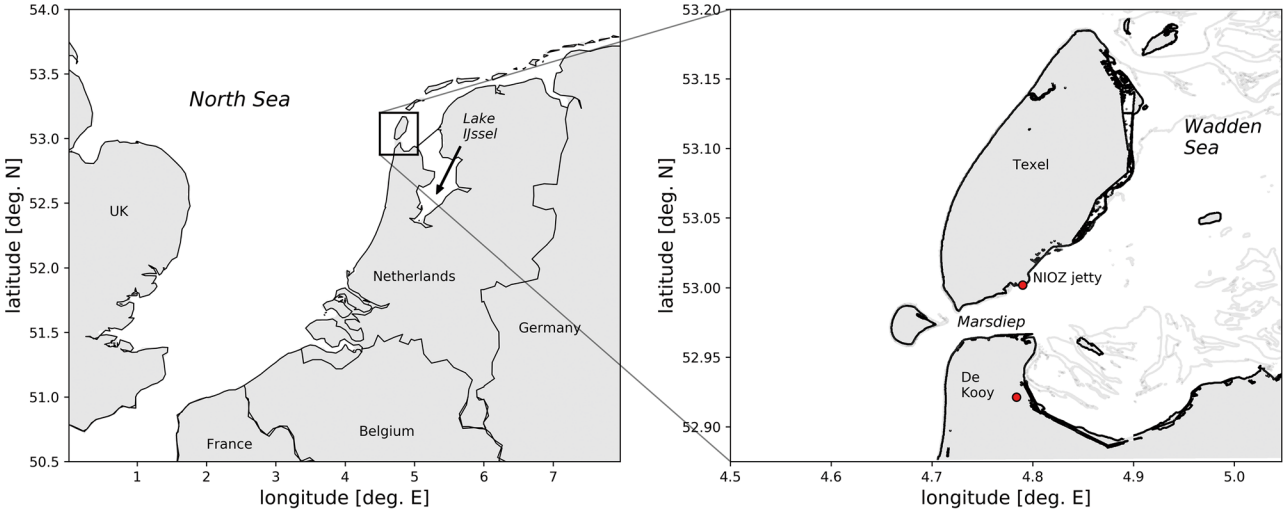

Fig. 1. Study area, including locations of the Royal Netherlands Institute for Sea Research (NIOZ) jetty sampling station, the Marsdiep tidal inlet, the Royal Netherlands Meteorological Institute weather station 'De Kooy' and the artificial freshwater Lake IJssel. Grey lines in the right panel: 1 m depth contour

mance liquid chromatography (HPLC) according to Evans et al. (1975). Total dissolved inorganic carbon (DIC) was measured by potentiometric titration. The underwater light attenuation (k_d) was derived directly using 2 spherical underwater quantum (photosynthetically active radiation, PAR) sensors: 'PAR_1' and 'PAR_2' (LI-COR LI-193), placed at 1.55 m (the highest distance possible due to tidal height) and 2.05 m depth at the jetty:

$$k_d = \ln\left(\frac{PAR_1}{PAR_2}\right) / z \quad (1)$$

where z is depth (m). Due to the relative turbidity of the area, sensors were placed within a relatively short distance from each other. This distance has proven to allow for accurate estimates of k_d. Data from these 2 PAR sensors was available only for part of 2014 and 2015. For the period of interest, 2012–2014, only Secchi disk depths (Z_{SD}; m) were available throughout. Therefore, first an empirical relationship between k_d and Z_{SD} was derived following the theoretical relation by Holmes (1970), using data from 2014 and 2015:

$$k_d = \frac{a}{Z_{SD}} + b \quad (2)$$

where $a = 1.476$ (unitless) and $b = 0.3541$ (unitless). The value of a was within the range found for other coastal waters (Lee et al. 2018). This relationship (n = 40, r^2 = 0.63) was used to estimate light attenuation from Z_{SD} for all sampling dates in the period 2012–2014 in the Marsdiep area.

Mixing depth (Z_{mix}; m) was set equal to the average depth of the Marsdiep basin (4.6 m) since the water column is mixed for most of the time (Nauw et al. 2014) and the euphotic depth (Z_{eu}; m) is defined as the depth at which 1% of the light measured at the surface penetrated:

$$Z_{eu} = \frac{\ln\left(\frac{100}{1}\right)}{K_d} \quad (3)$$

Hourly values of irradiance (i.e. PAR) just above the water surface (E_{PAR+0}; µmol photons m^{-2} h^{-1}; 400–700 nm) were measured at the jetty (TriOS RAMSES ACC). In case of missing values, data on average hourly irradiance (E_0; J cm^{-2}) were taken from the Royal Netherlands Meteorological Institute (KNMI) station at the 'De Kooy' airport (Fig. 1) and converted to µmol photons m^{-2} s^{-1} PAR using an empirical relationship derived by comparing light measurements from the sensor at the jetty to data from the 'De Kooy' station ($E_{PAR+0} = E_0 \times 5.95$; n = 8760, $r^2 = 0.94$).

Samples for dissolved inorganic nutrient analysis were filtered over a 0.22 µm polycarbonate filter and stored until analysis at –20°C (for N and P) or 4°C (for Si). Nutrient concentrations were analysed at the NIOZ using a Traacs 800 auto-analyser (Technicon). To explore the variation in and correlation between environmental variables, a principal component analysis (PCA) was performed using the R library 'vegan' (R Core Team 2018). For all analyses, R version 3.5.1 was used. Variables were normalised before analysis.

2.2. Carbon fixation measurements

A sample of 90 ml was spiked with 2.25 ml $NaH^{14}CO_3^-$ with an activity of approximately 1 Mbq ml^{-1}; the sample was gently mixed and divided over 23 incubation flasks holding 4.1 ml each. The actual activity added per incubation was determined by measuring the activity of the flask with 100 µl $NaH^{14}CO_3^-$ added to 4 ml of 1 M NaOH. This flask served as the 'control' and was not incubated but was closed and placed under the fume hood. The 22 flasks with spiked seawater were placed in a photosynthetron (CHPT, model TGC1000, equipped with 2 halogen light bulbs: Philips 13095, 250 W) and incubated for 2 h at *in situ* temperatures (Lewis & Smith 1983). The incubation temperature was controlled by a water bath; temperatures in the incubator were measured before and directly after the incubation. Despite the use of the water bath, temperatures deviated from *in situ* temperatures occasionally. In those instances, a correction factor (T_{corr}, °C) was applied, with $T_{corr} = e^{0.0693} \times (T_{in\ situ} - T_{incubation})$. Differences between $T_{in\ situ}$ and $T_{incubation}$ (average of temperature at the start and the end) varied between 0.4 and −4.2°C.

Two flasks of the 22 were covered with aluminium foil, receiving no light. The radioactivity measured in these samples after incubation served as the 'dark' value and was subtracted from the samples incubated in the light.

Directly after incubation, 100 µl of concentrated (37%) HCl was added to each flask (except the control) to halt further uptake of bicarbonate; the incubation flasks remained under the fume hood to degas for 24 h. Scintillation fluid (Ultima Gold) was added and analysis of radioactivity (disintegrations min^{-1}, dpm) was carried out using a scintillation counter (PerkinElmer, Tri-Carb 2910TR).

Light at each position in the photosynthetron was measured inside the incubation flasks using a light meter (WALZ ULM-500) with spherical micro sensor (US-SQS/L). Light levels received (E_s) ranged from 0 to a maximum of 1700 µmol photons m^{-2} s^{-1} (PAR) depending on the position of the flask in the photosynthetron. The carbon fixation rate (i.e. P; mg C l^{-1} h^{-1}) per sample was calculated as:

$$P = \left(\frac{(dpm_{sample} - dpm_{avg\_dark}) \times DIC \times 1.05 \times T_{corr}}{dpm_{added} \times t} \right) \quad (4)$$

where dpm_{added} is the dpm as measured in the control bottle, t is the duration of the incubation (in h), and 1.05 is a correction factor for the preference of the enzyme RUBISCO for the ^{12}C atom over the ^{14}C atom. For sampling dates in 2013 and 2014, DIC was estimated using titration (Strickland & Parsons 1972); no data on DIC concentrations were available for 2012. For 2013 and 2014, there was no clear seasonal trend, and average values did not significantly differ between these 2 yr (2013: 26.7 ± 1.0 mg l^{-1}, 2014: 25.2 ± 1.6 mg l^{-1}). Therefore, the median DIC for the period 2013–2014 of 26.0 mg l^{-1} was used for all calculations in 2012, 2013 and 2014. P was then divided by the chl *a* concentration of the sample to obtain chlorophyll-specific fixation rates (i.e. P^B; mg C [mg chl *a*]$^{-1}$ h^{-1}). Recent research has indicated that the ^{14}C method gives an approximation of net production for most species (Pei & Laws 2013). However, research by Halsey et al. (2010, 2013) and Milligan et al. (2015) clearly demonstrated that the algal growth rate is the factor that determines whether short-term incubations measure net or gross photosynthesis (or something in between).

2.3. *P–E* curve fitting

P^B rates were used to construct *P–E* curves and to estimate the photosynthetic parameters from the curves according to 4 models: those of Eilers & Peeters (1988) (EP), Jassby & Platt (1976) (JP), Platt et al. (1980) (PGH) and Webb et al. (1974) (Webb). Although these models originally used different functions and defining parameters, similar photosynthetic parameters can be derived for the models excluding photo-inhibition (parameters P^B_{max}, α^B) and those including photo-inhibition (P^B_{max}, α^B, β^B) (Fig. 2, see Table 1).

Estimation of the photosynthetic parameters for biomass-specific carbon fixation (i.e. P^B_{max}, β^B) of these 4 models was performed using the R library 'phytotools' (Silsbe & Malkin 2015, R Core Team 2018). For all models, the lower limit of 0.0 for estimation of the parameters (performed by 'phytotools') was insufficient: despite the parameters being positive, small negative values were needed within the iterative process to arrive at the best parameter estimation for this data set. Thus, lower limits were adjusted to −1.0. In order to compare photo-inhibition effects between the PGH and EP models, the photo-inhibition slope (i.e. β^B; mg C l^{-1} h^{-1} [µmol m^{-2} s^{-1}]$^{-1}$) was defined as the downward slope between the optimal light intensity and twice the optimal light intensity (Fig. 2). Note that a positive value of β^B therefore indicates that photo-inhibition is occurring.

The EP model includes the term E_{opt} (E_{max} in our Fig. 2), which describes the irradiance at which photosynthesis reaches its maximum value before it

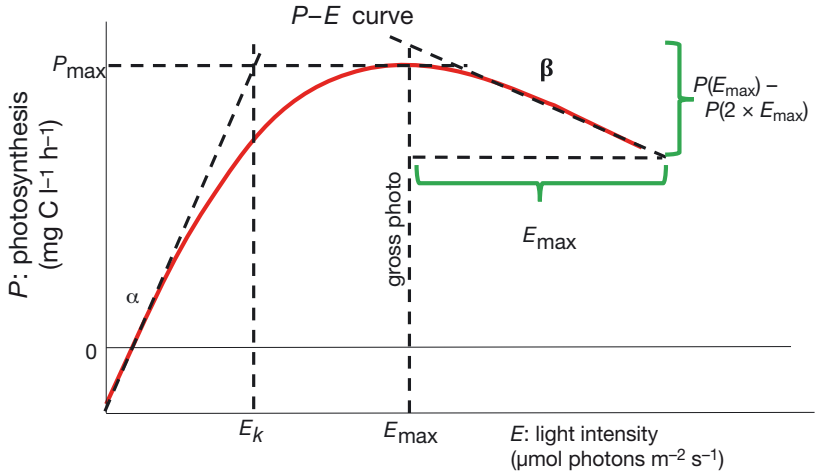

Fig. 2. Conceptual *P–E* curve, with various parameters that define the photosynthetic response of the sample's phytoplankton to increasing light intensities. Photo-inhibition is defined as $\beta = P(E_{max}) - P(2 \times E_{max}) / E_{max}$ to allow for a comparison of possible photo-inhibition between models. Note that β is defined as a positive, downward slope, to allow for comparison with other photo-inhibition parameters. P_{max} is the maximum fixation rate (mg C l^{-1} h^{-1}), α the initial slope of the *P–E* curve (mg C l^{-1} h^{-1} [µmol photons m^{-2} s^{-1}]$^{-1}$), E_k the light saturation coefficient (µmol photons m^{-2} s^{-1}), calculated as P_{max}/α, and β (mg C l^{-1} h^{-1} [µmol photons m^{-2} s^{-1}]$^{-1}$) the photo-inhibition parameter. E_{max} is the light intensity (µmol photons m^{-2} s^{-1}) at which P_{max} is reached

declines again because of photo-inhibition. This model is the only one of the 4 models used in the current paper that is based on a mechanistic description of the photosynthetic process. The photosynthetic parameters α and P_{max} are derived from the fit-coefficients *a*, *b* and *c*. The EP model has been reformulated by Herlory et al. (2007) so that the fit-parameters α and P_{max} can be derived directly from the *P–E* data (see Table 1).

In the PGH model, P_s equals P_{max} when there is no photo-inhibition ($\beta^B = 0$). If $\beta^B > 0$, then $P_s > P_{max}$, and P_s can be interpreted as the 'maximum photosynthesis output that could be sustained if there were no β' (Platt et al. 1980). The parameter $E_k = P_{max} / \alpha$ (Talling 1957) is the saturating irradiance (the inflection point where photosynthesis becomes saturated) (Fig. 2). This parameter gives an indication of light–shade adaptation characteristics (Falkowski & Raven 2007) and estimated values for E_k provide information on the light acclimation status of the phytoplankton community.

The results of the curve fits were compared between models based on the smallest squared sum of the residuals (SSR) (Spiess & Neumeyer 2010). Because the models including photo-inhibition are more complex (3 photosynthetic parameters) than the ones without (2 photosynthetic parameters), model selection was also done by using Akaike's information criterion (AIC), which deals with the trade-off between the goodness of fit of the model and its simplicity (Burnham & Anderson 2004).

Covariance between the estimates of the photosynthetic parameters was checked by Pearson correlation. The results of the model that gave the best fit were used to explore possible reasons for the observed seasonal and year-to-year variation in the photosynthetic parameters.

2.4. Calculation of daily and annual production

Daily production estimates for the water column (mg C m^{-2} d^{-1}) for sampled days were based upon the photosynthetic parameters from all 4 models, hourly values of irradiance in PAR (from the jetty and, in case of missing values, from the nearest KNMI station, 'De Kooy') and k_d. Maximum water depth for which production was calculated was fixed at 4.6 m. Irradiance in the water column just under the water surface ($E_{PAR\text{-}0}$; µmol photons m^{-2} h^{-1}) was corrected for reflectance at the water surface (7%; Højerslev 1978, cf. Philippart et al. 2007). Daily estimates of primary production were made using the 'phytotools' package (Silsbe & Malkin 2015, R Core Team 2018, present study) by integration of the fitted curve over depth and time (24 h). Primary production on non-sample days was calculated in the same way, using observed hourly irradiance values together with linearly interpolated values for k_d (m^{-1}), chl *a* concentration (µg chl l^{-1}) and the photosynthetic parameters P^B_{max} and α^B (and possibly β^B). Thus, an estimation was made of the *P–E* curve parameters on a non-sample day based on the curve parameters of the surrounding sample days, thus defining the *P–E* curve used for integration to daily primary production on the non-sample day. Annual production (g C m^{-2} yr^{-1}) was estimated by adding up all daily primary production values of the year (including a leap day for 2012).

2.5. Relationships between photosynthetic parameters and environmental conditions

Results of the best *P–E* model were subsequently used to explore relationships between parameter values and environmental conditions, focussing on those variables that could be obtained from Earth Observa-

tion data. Estimated values of α^B and P^B_{max} were correlated to the environmental variables, and only variables that were significantly correlated ($p < 0.05$) were used in the multivariate model. Three models were explored, one with year as a factor (Model a), one without year as a factor (Model b) and one model where extreme values of the *P–E* parameters were removed (Model c). Extreme values were defined as (values − mean) > 3 × SD. From the full model, variables were subsequently removed when they did not significantly add to the explained variance.

3. RESULTS

3.1. Environmental conditions

There were considerable differences in environmental conditions between years (Fig. 3). The year 2013 had a median SST of 11.9°C (Fig. 3A), and was relatively cold compared to 2012 (14.6°C) and 2014 (15.8°C). In 2013, the water temperature remained relatively low (e.g. <5°C) until mid-April (Fig. 4). The highest maximum water temperature was recorded in 2014 (22.1°C), while the highest temperatures in 2012 and 2013 were 20.4 and 20.2°C, respectively (Figs. 3A & 4).

The timing of the onset of the spring bloom, defined as a daily increase in chl *a* concentration above 0.2 µg l^{-1} d^{-1} (Philippart et al. 2007), was remarkably similar across the 3 yr, with an estimated onset in the second week of March in each year (day of the year 72, 71 and 69 in 2012, 2013 and 2014, respectively). Peak chl *a* concentrations for the spring bloom were 25.4, 21.0 and 21.5 µg l^{-1} in order of years. In 2012, there was a second peak in the chl *a* concentration of 27.8 µg l^{-1} on Day 194 (23 July) (Fig. 5). The median concentration of phytoplankton was 4.6 µg chl *a* l^{-1}. In 2013 (the

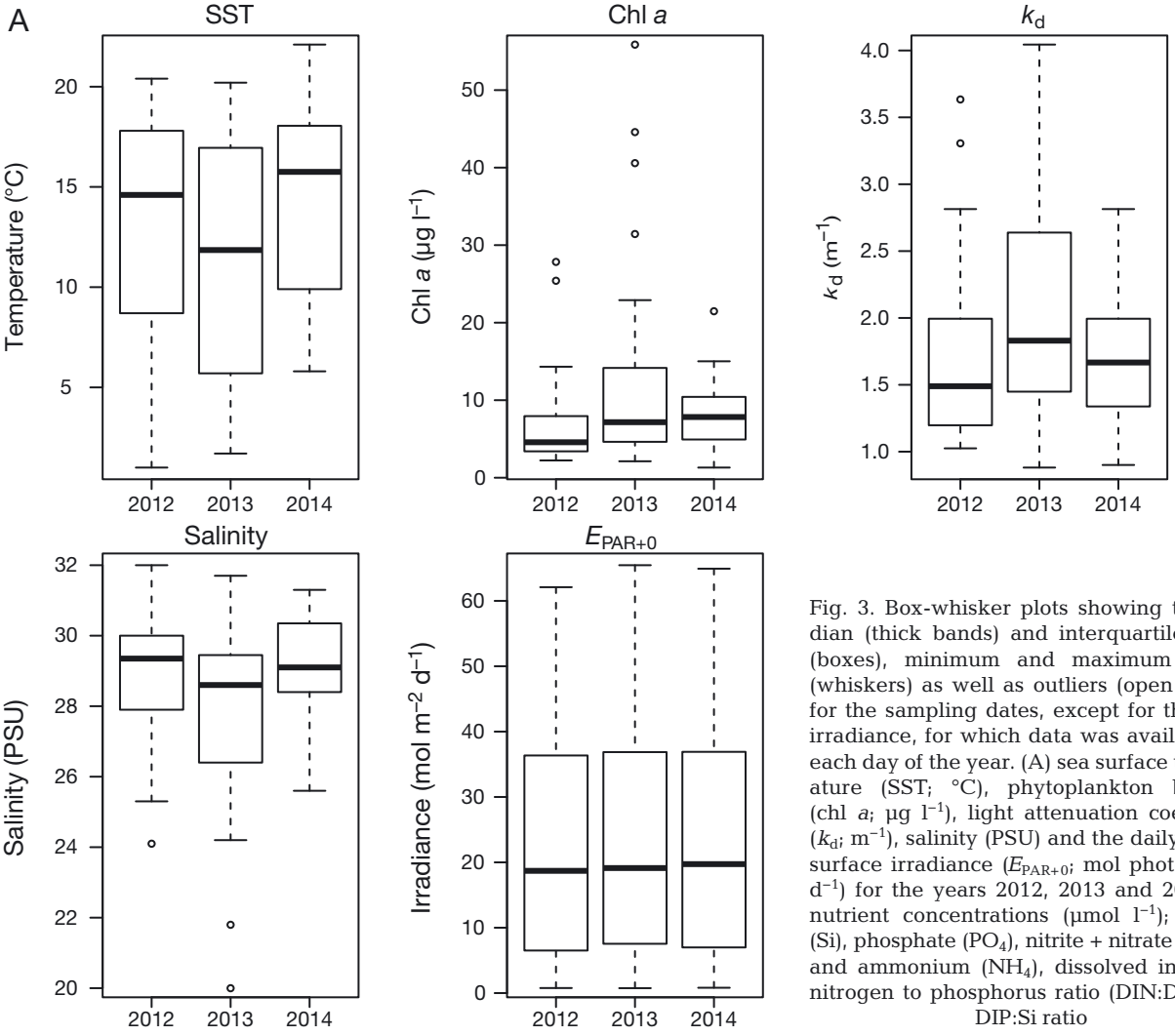

Fig. 3. Box-whisker plots showing the median (thick bands) and interquartile range (boxes), minimum and maximum values (whiskers) as well as outliers (open circles) for the sampling dates, except for the daily irradiance, for which data was available for each day of the year. (A) sea surface temperature (SST; °C), phytoplankton biomass (chl *a*; µg l^{-1}), light attenuation coefficient (k_d; m^{-1}), salinity (PSU) and the daily sum of surface irradiance (E_{PAR+0}; mol photons m^{-2} d^{-1}) for the years 2012, 2013 and 2014; (B) nutrient concentrations (µmol l^{-1}); silicate (Si), phosphate (PO_4), nitrite + nitrate (NO_{2+3}) and ammonium (NH_4), dissolved inorganic nitrogen to phosphorus ratio (DIN:DIP) and DIP:Si ratio

Fig. 3 continued on next page

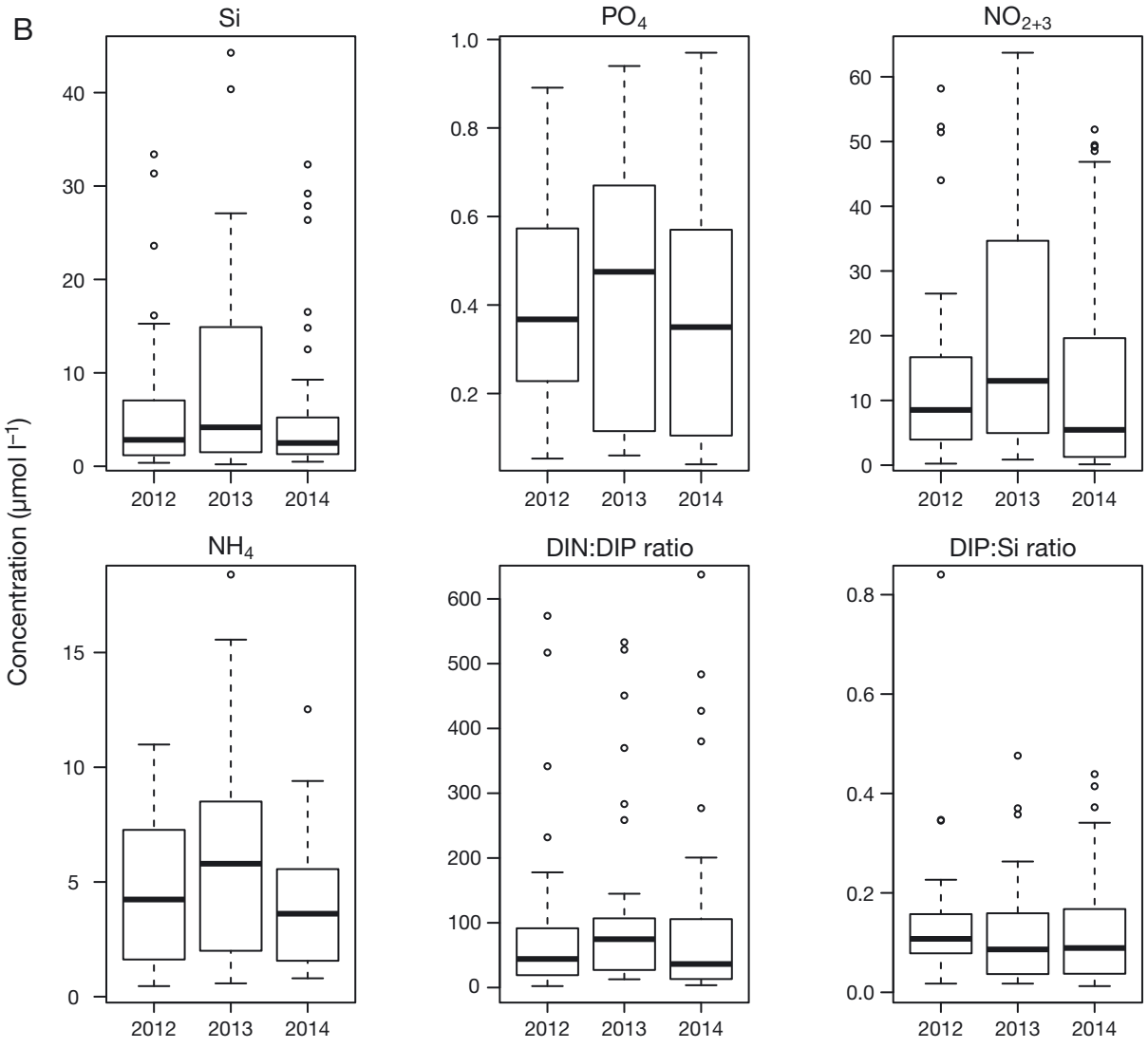

Fig. 3 (continued)

coldest year), the bloom lasted longer; there were several peaks in chl *a* concentration, with a maximum concentration of 55.9 µg l^{-1} on Day 147 (27 May). The median concentration in 2013 of 7.2 µg l^{-1} was higher than in 2012, but lower than in 2014 (7.8 µg l^{-1}) (Fig. 3A). In 2013, chl *a* concentrations decreased from Day 175 (24 June) onwards until Day 204, when there was another peak. In 2012, there was a last peak at day 194 (12 July). In 2014, a peak in summer was absent, and this was the only year with a small autumn bloom (Day 267; 24 September).

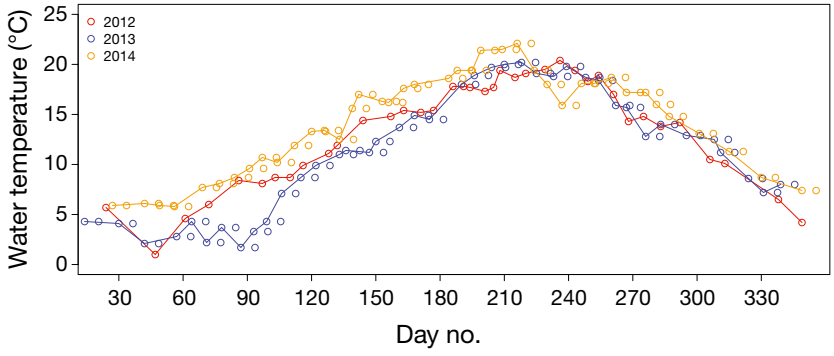

Fig. 4. Sea surface temperature (SST; °C) at the Marsdiep jetty in 2012, 2013 and 2014

Values of k_d ranged from 0.88–4.0 m^{-1} (Fig. 3A), with median values highest in 2013 (1.83) compared to 2012 (1.49) and 2014 (1.67). From 2012–2014, Z_{eu} ranged from 1.1–5.2 m. The ratio between Z_{eu} and Z_{mix} was between 0.2 and 1 for most sampling dates, indica-

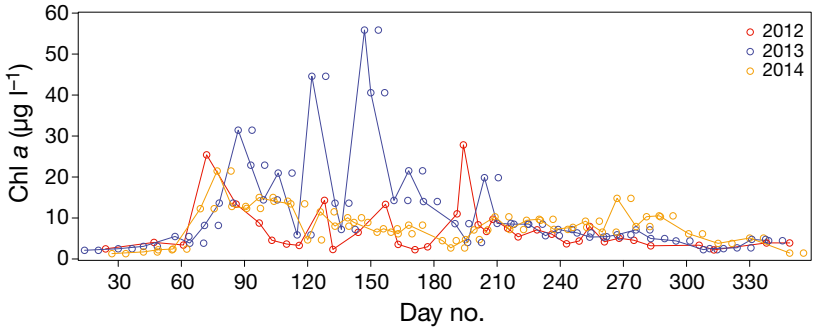

Fig. 5. Chl *a* concentration (µg l^{-1}) at the Marsdiep jetty in 2012, 2013 and 2014

ting that there was positive net productivity, but over a depth smaller than the average water depth. Median salinity values differed little between years (29.4, 28.6 and 29.1 respectively for 2012, 2013 and 2014).

There were clear seasonal patterns in nutrient concentrations (Section 1, Fig. S1 in the Supplement at www.int-res.com/articles/suppl/m639p053_supp.pdf), with the highest average concentrations in winter. The concentration of silicate and PO_4 (µmol l^{-1}) decreased sharply from Day 60 to 90, corresponding with the time of phytoplankton bloom. The concentration of dissolved nitrogen (DIN [NO_3, NO_2 and NH_4], µmol l^{-1}) declined as well, but at a lower magnitude. Silicate (Si) concentrations remained low until September. The lowest concentration for PO_4 was found in April, while for DIN lowest concentrations were found in August. Redfield ratios of nutrients, combined with absolute concentrations, can provide information about the nutrient, or combination of nutrients that are limiting phytoplankton biomass (Redfield 1958). A DIN: dissolved inorganic phosphorus (DIP) ratio >16 indicates P-limitation, while DIN:DIP < 16 indicates N-limitation. However, as long as concentrations exceed 21–36 µmol l^{-1} for DIN and 0.16 µmol l^{-1} for DIP, then neither nutrient is considered limiting (Redfield 1958, Ekholm 2008). For diatoms, a DIP:Si ratio above 0.07 indicates silicate limitation (Redfield 1958 in Ekholm 2008). In the current study, the Redfield ratio of DIN:DIP was found to be <16 occasionally in the months of July–September, while the ratio of DIP:Si was above 0.07 from April–October. Combined with the absolute concentrations measured, it can be concluded that for the years 2012–2014 at the Marsdiep jetty, N was limiting phytoplankton biomass in summer, while the rest of the year there was a co-limitation of DIP and silicate (Supplement Section 1, Fig. S1). With regard to the differences between years, it can be seen that variations in nutrient concentrations were higher in 2013 compared to the other 2 yr (Fig. 3B).

Results from the PCA analysis showed that the first 2 principal components (PCs) of the environmental factors accounted for 67% of the total variance of the normalised environmental data. Co-variability among environmental factors was relatively high because the explained variance was higher than the minimum value of the variance explained by the first 2 PCs in the event all 9 factors were uncorrelated (i.e. 2/9 = 22%). Most variance in the environmental data set was found in SST, silicate and NO_{2+3} concentrations. In late winter, low temperatures and salinity co-occurred with relatively turbid and NO_{2+3}-rich waters. From spring until the start of summer, high chl *a* concentrations co-occurred with low PO_4 and NH_4 concentrations, followed by the highest values of daily insolation, which coincided with low silicate concentrations. The highest water temperatures were found at the end of summer, which co-occurred with the highest salinities and relatively clear and NO_{2+3}-poor waters. Finally, from early to mid-winter, low chl *a* concentrations were found which co-occurred with high PO_4 and NH_4 concentrations, followed by the lowest values of daily insolation, which coincided with high silicate concentrations.

3.2. *P–E* curves

For 2012, 2013 and 2014, a total of 107 incubations were performed. For these days, *P–E* curves were fitted using 4 models (Table 1, Fig. 6): EP, JP, PGH and Webb. The results of curve fits were compared among models using the SSR and AIC. Both the distribution of SSR and AIC scores were quite similar for the 4 models, but the Webb model had the highest SSR for all curve fits. A closer look at the differences in SSR between models revealed that especially at small values for SSR (<20) the Webb, EP and PGH models had a systematically higher SSR compared to JP. In addition, for each *P–E* curve fit it was determined which model had the lowest SSR, highest SSR and lowest AIC score (Table 2); based on these counts, it was decided that JP was the best model for this data set, with the lowest SSR and AIC for most fits (51 and 75 out of 107, respectively).

The estimates of α^B and P^B_{max} were compared between models (Table 3). With the PGH model, α^B could not be estimated for 2 incubations and P^B_{max} could not be estimated on 16 occasions. Depending on

Table 1. Four models used to fit the relationship between carbon fixation rates (P; mg C l^{-1} h^{-1}) and irradiance (E; µmol photons m^{-2} s^{-1}). P_{max} is the maximum fixation rate (mg C l^{-1} h^{-1}), α the initial slope of the P–E curve (mg C l^{-1} h^{-1} [µmol photons m^{-2} s^{-1}]$^{-1}$), E_k the light saturation coefficient (µmol photons m^{-2} s^{-1}) and β (mg C l^{-1} h^{-1} [µmol photons m^{-2} s^{-1}]$^{-1}$) the photo-inhibition parameter. The EP model uses the parameters a, b and c, which can be derived from α, P_{max} and E_{max}, which is the light intensity (µmol photons m^{-2} s^{-1}) at which P_{max} is reached. Equations and derived parameters were taken from the original papers, as well as from Arbones et al. (2000), Macedo et al. (1998) and Frenette et al. (1993)

Model	No. of parameters	Reference	Original equation	Derived parameters
EP	3	Eilers & Peeters (1988)	$P = \frac{E}{aE^2 + bE + c}$	$\alpha = \frac{1}{c}$, $P_{max} = \frac{1}{b + 2\sqrt{ac}}$
		Herlory et al. (2007)	$P = \frac{E}{\frac{E^2}{\alpha E_k^2} + \frac{E}{P_{max}} - \frac{2E}{\alpha E_k} + \frac{1}{\alpha}}$	
JP	2	Jassby & Platt (1976)	$P = P_{max} \tanh\left(\frac{\alpha E}{P_{max}}\right)$	
PGH	3	Platt et al. (1980)	$P = P_s\left[1 - \exp\left(\frac{-\alpha E}{P_{max}}\right)\right]\exp\left(\frac{-\beta E}{P_s}\right)$	$P_{max} = P_s\left[\frac{\alpha}{\alpha+\beta}\right]\left[\frac{\beta}{\alpha+\beta}\right]^{\beta/\alpha}$
Webb	2	Webb et al. (1974)	$P = P_{max}\left[1 - \exp\left(\frac{-\alpha E}{P_{max}}\right)\right]$	

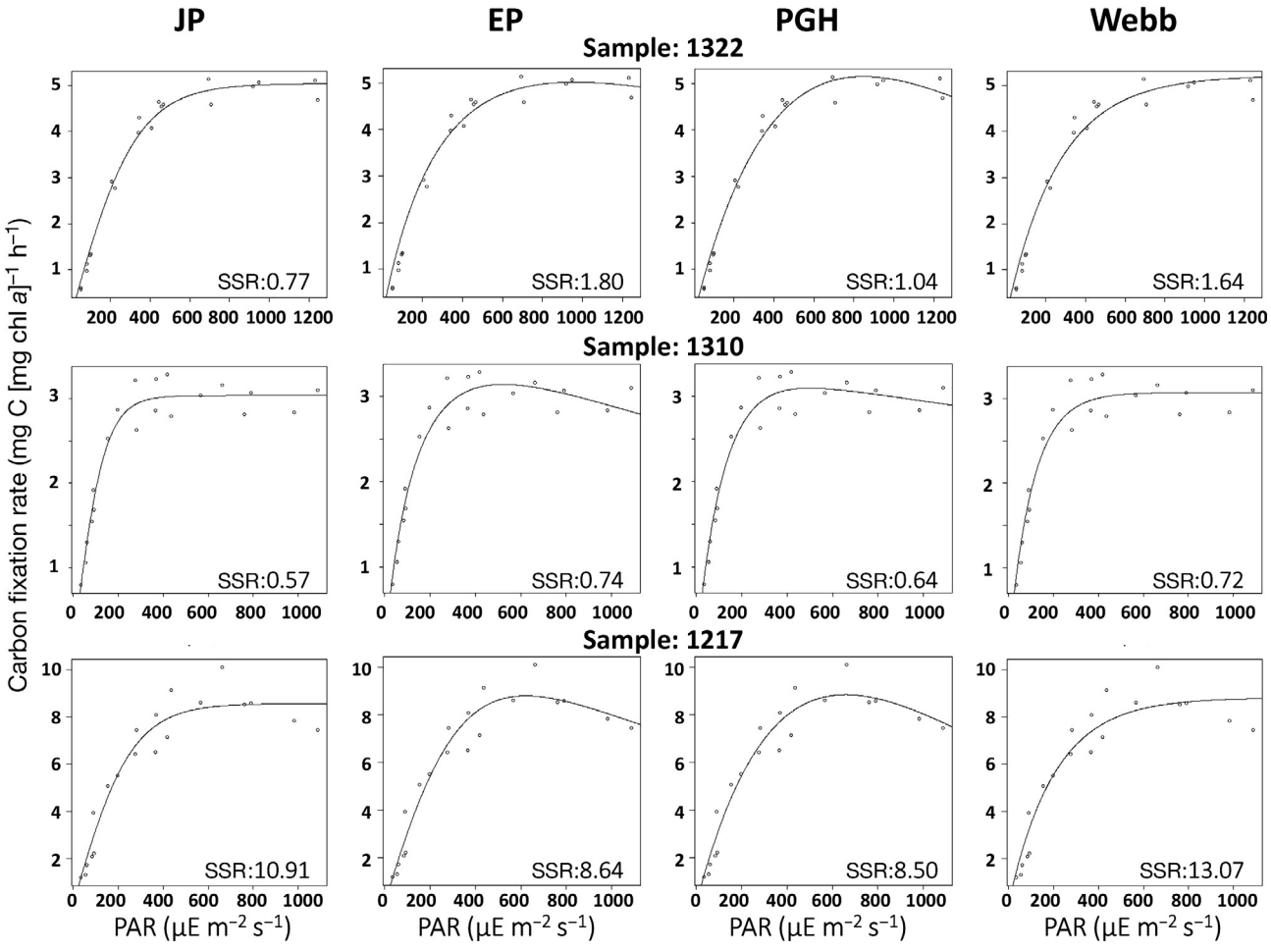

Fig. 6. Four models were applied to the data; 2 without photo-inhibition (JP and Webb) and 2 with photo-inhibition (EP and PGH) (see Table 1 for model details). Examples of P–E curves derived from each of these models are shown for 3 dates: 15 July 2013 (sample no. 1322), 9 April 2013 (1310) and 19 June 2012 (1217). SSR: smallest squared sum of residuals

Table 2. Squared sum of the residuals (SSR) of the *P–E* curve fit for the different models. The number of incubations in the period 2012–2014 was 107; per model, the number of times this model had the lowest SSR and the number of times the model fit yielded the highest SSR is given. The percentage of the times a model had the lowest Akaike's information criterion (AIC) value is also given

Model	Smallest SSR	Highest SSR	% lowest AIC
EP	35	28	8
JP	51	10	75
Webb	3	60	14
PGH	18	9	3

the model choice, the average estimate for α^B was 28% higher with Webb, and 19% for PGH and EP compared to JP. For P^B_{max} estimates, both EP and PGH gave estimates that were on average 2% higher compared to JP; for Webb this was on average 5%. Models EP and PGH allowed for a fit including photo-inhibition, and the estimates of β^B as defined in this study (see Section 2.3) for both models resulted in a good correlation (r = 0.94). For PGH, β^B could be estimated for 90 incubations, and for EP this was 106 times. The estimated β^B from PGH was on average 10% lower compared to the estimated β^B from EP. The average estimate of β^B for EP was 0.0015 ± 0.0015 mg C [mg chl *a*]$^{-1}$ h^{-1} (µmol photons m^{-2} s^{-1})$^{-1}$.

3.3. Temporal variation in photosynthetic parameters

To investigate the seasonal and year-to-year variation in photosynthetic parameters, results from the JP model were used. Values ranged between 0.00024 and 0.24 mg C [mg chl *a*]$^{-1}$ h^{-1} (µmol m^{-2} s^{-1})$^{-1}$ for α^B with median values of 0.038, 0.019 and 0.016 in 2012,

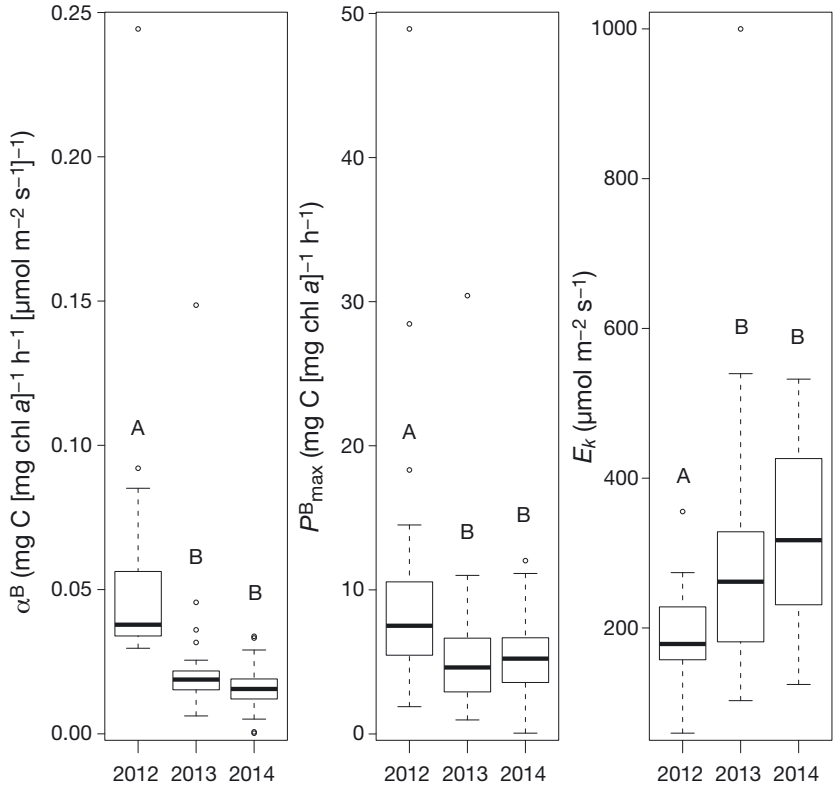

Fig. 7. Box-whisker plots of the variation per year in estimates for α^B (mg C [mg chl *a*]$^{-1}$ h^{-1} [µmol m^{-2} s^{-1}]$^{-1}$), P^B_{max} (mg C [mg chl *a*]$^{-1}$ h^{-1}) and E_k (µmol m^{-2} s^{-1}) using *P–E* curve fits from the JP model. See Fig. 3 for box-plot parameter definitions. Different letters indicate significant difference ($p < 0.05$) between years

Table 3. Estimates for α^B (mg C [mg chl *a*]$^{-1}$ h^{-1} [µmol m^{-2} s^{-1}]$^{-1}$) and P^B_{max} (mg C [mg chl *a*]$^{-1}$ h^{-1}) relative to the estimate from model fit according to: JP = *aX* + *b*, where *X* is either α^B or P^B_{max} from the EP, PGH or Webb models (see Table 1 for model specifics). For both the intercept (*b*) and regression coefficient (*a*), the average ± SD value is given as well as the p-value (ns: not significant: $p > 0.05$). R^2: explained variance of the regression

	Model	Regression coefficient	p	Intercept	p	R^2
α^B	EP	1.19 ± 0.05	<0.0001	0.0022 ± 0.0020	ns	0.853
	Webb	1.28 ± 0.01	<0.0001	0.0005 ± 0.0003	ns	0.996
	PGH	1.19 ± 0.01	<0.0001	0.0009 ± 0.0006	ns	0.984
P^B_{max}	EP	1.02 ± 0.01	<0.0001	0.17 ± 0.05	0.0003	0.996
	Webb	1.05 ± 0.01	<0.0001	−0.09 ± 0.04	0.04	0.998
	PGH	1.02 ± 0.00	<0.0001	0.03 ± 0.03	ns	0.999

2013 and 2014, respectively (Fig. 7). Values for α^B were always higher in 2012 compared to the values in 2013 and 2014, except for one outlier in 2013. Values showed little variation in 2014; this year also had the lowest absolute estimates for α^B (Figs. 7 & 8).

P^B_{max} estimates varied between 0.1 and 48.9 mg C (mg chl *a*)$^{-1}$ h^{-1} with median values of 7.5, 4.6 and 5.2 for the 3 yr (Fig. 7). Both the absolute and median estimates for P^B_{max} were highest in 2012 compared to the other 2 yr (Figs. 7 & 8). In 2014, the lowest absolute values for P^B_{max} were found. Apart from the outliers, there was a general increase in the value of P^B_{max} from the end of spring to the end of September (Day 270). In 2013, low values for the first months of the year (up until Day 110, end of April) corresponded to low water temperatures in the same period (Fig. 4). In 2012, there was a peak in estimates for both α^B and P^B_{max} in October and November (Days 283 and 306) (Figs. 7 & 8), which did not correspond to high chl *a* concentration, nor to high water temperature (Figs. 4 & 5). The estimates for P^B_{max} and α^B were highly correlated (Fig. 9) and α^B can be estimated from P^B_{max} from the linear relation $\alpha^B = 0.05 \pm 0.02 + 0.13 \pm 0.01 P^B_{max}$, explaining 64 % of the variance ($F_{1,105} = 188.4$, $p < 0.0001$). The parameter E_k (µmol m^{-2} s^{-1}), calculated as P^B_{max} / α^B, represents the irradiance at which light becomes saturating. Throughout the year, estimates for E_k were lowest for 2012. As for $P^B_{max,}$ there was an increase from spring towards autumn (Figs. 7 & 8).

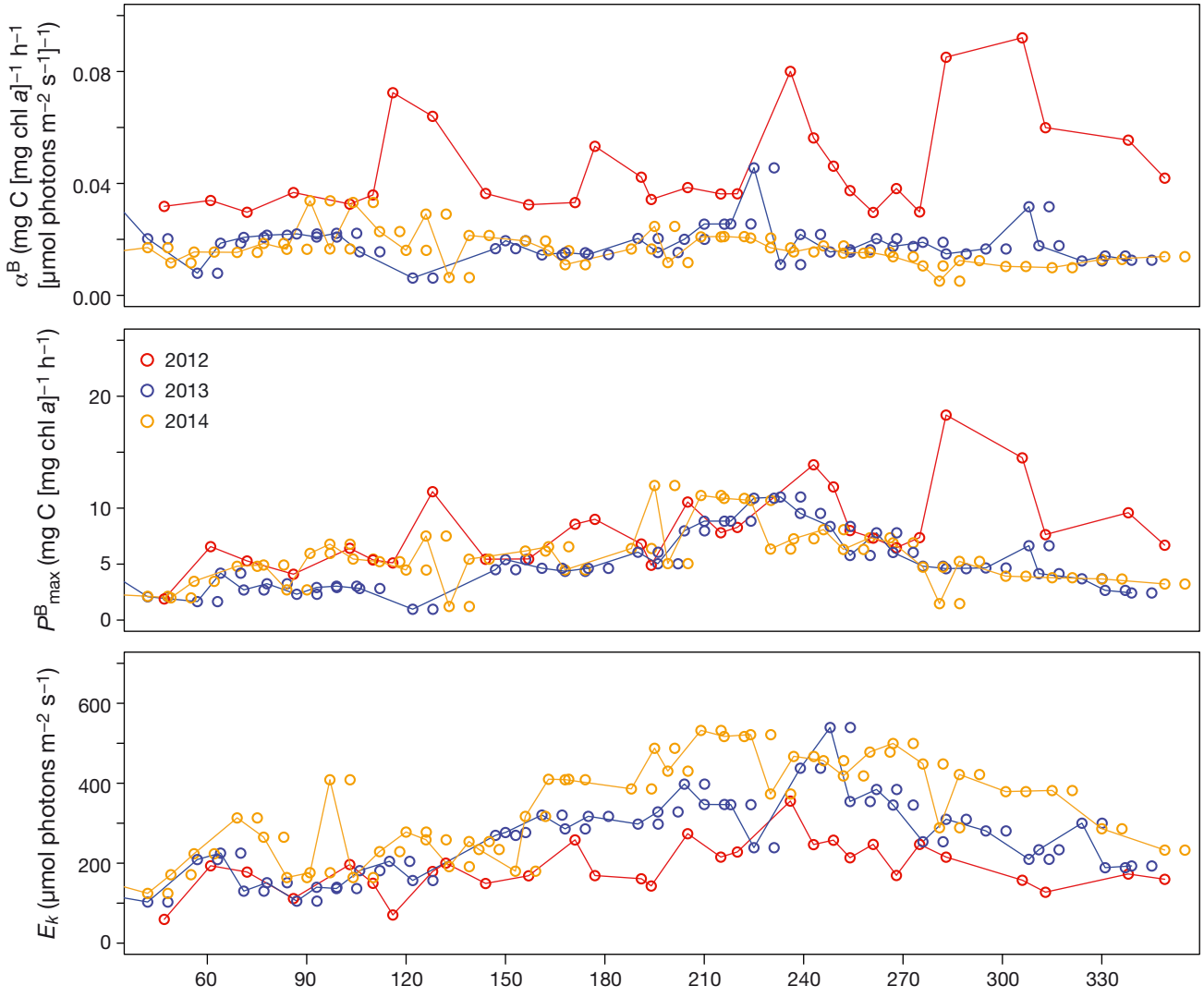

Fig. 8. Chl *a* normalised photosynthetic parameters α^B (mg C [mg chl *a*]$^{-1}$ h^{-1} [µmol photons m^{-2} s^{-1}]$^{-1}$) and P^B_{max} (mg C [mg chl *a*]$^{-1}$ h^{-1}) as well as E_k (µmol photons m^{-2} s^{-1}), as estimated by means of the JP model at the Marsdiep jetty in 2012, 2013 and 2014. Note that outliers (see Section 2.5) were removed for better visualisation of the seasonal pattern of photosynthetic parameters

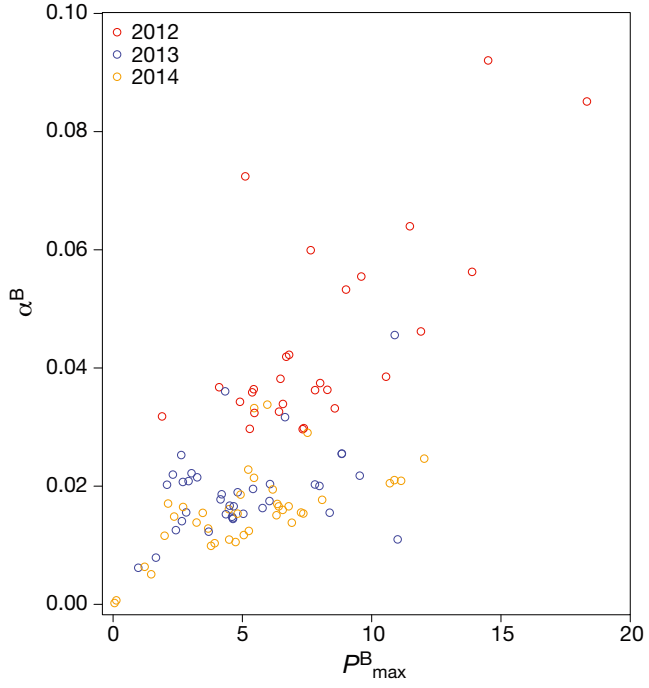

Fig. 9. Relationship between α^B and P^B_{max} (as estimated by means of the JP model) at the Marsdiep jetty in the years 2012, 2013 and 2014. Outliers for α^B and P^B_{max} were omitted for clarity (see Section 2.5)

3.4. The relation of photosynthetic parameters with environmental parameters

For α^B, there was no significant univariate correlation with any of the environmental variables (Fig. 10). P^B_{max} correlated positively with SST and negatively with NO_{2+3}, silicate and k_d (Fig. 10) when all years were analysed together. These variables were included in the multivariate linear models. Adding year as a factor to the models always resulted in a lower AIC than similar models without the year effect (Supplement Section 2, Table S1).

The best model, based on the lowest AIC, was the model that included year and SST. The difference in AIC of this model compared to that of next best was 2 (Model 3b, Supplement Section 2, Table S1), indicating that these 2 models are comparable to each other (Burnham & Anderson 2004). In such a case, the simplest model should be considered. As long as it remains unknown which environmental condition(s) determine(s) this additional year-to-year variation, the best model to provide satellite-derived information for P^B_{max} is one that includes SST only. A model that includes SST and a model that includes both SST and silicate (Supplement Section 2) can describe the variation in E_k equally well.

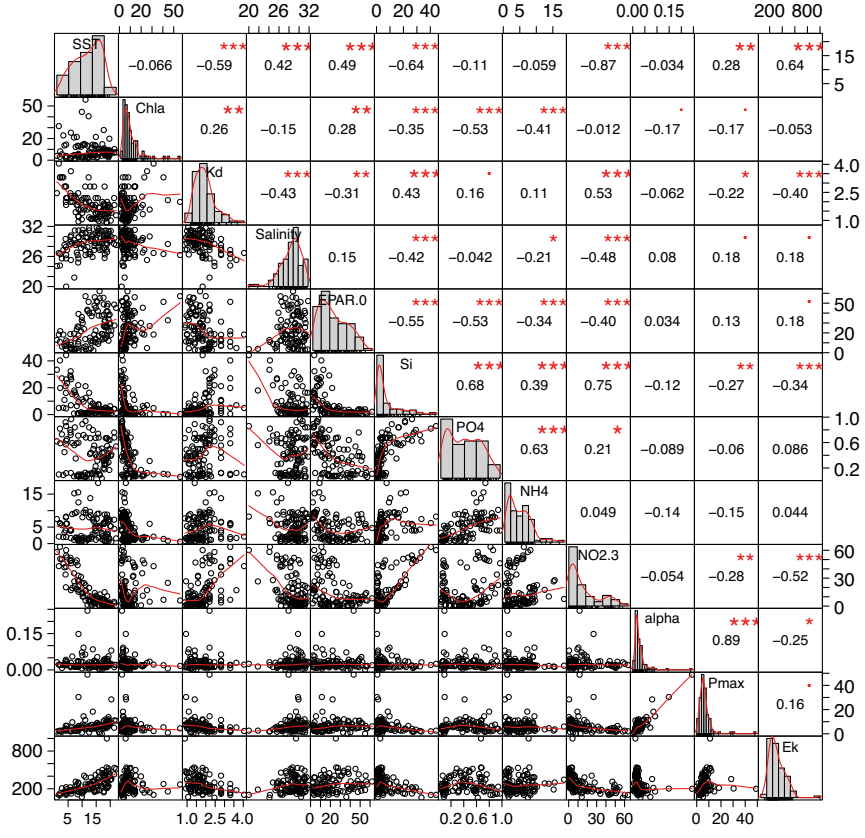

3.5. Daily and annual primary production

Estimates for daily water column production, using the JP model, ranged from to 3.4 mg to 3800 mg C m^{-2} d^{-1}, with large differences between the 3 yr (Fig. 11). Average daily production was 0.54, 0.65 and 0.36 g C m^{-2} d^{-1} in 2012, 2013 and 2014, respectively. For 2012, 2013 and 2014, annual production was

Fig. 10. Correlations between environmental variables measured at the Marsdiep jetty in the years 2012, 2013 and 2014 and the photosynthetic parameters α^B, P^B_{max} and E_k. The distribution of each variable is shown on the diagonal. On the bottom of the diagonal, the bivariate scatter plots with a fitted line are displayed, on the top of the diagonal the value of the correlation plus the significance level as a symbol are displayed; the symbols '***', '**', '*', '.', ' ') correspond to p-values (0, <0.001, <0.01, <0.05 and >0.1)

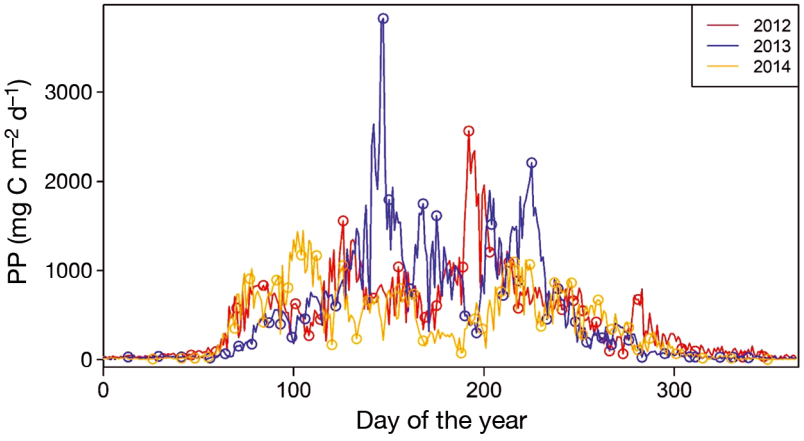

Fig. 11. Estimates of daily column integrated primary production (PP) at the Marsdiep jetty in 2012, 2013 and 2014. The open circles indicate the sampling dates. The estimates were made using the curve fit from the JP model. (See Section 2.4 for details of calculation and integration procedure)

198, 239 and 131 g C m^{-2} yr^{-1}, respectively (Table 4). When estimates of yearly production based on curve fits from the JP model were compared with estimates based on the EP, PGH or Webb models, JP gave the lowest estimates except for one occasion (EP in 2013) (Table 4). Annual production estimates from the 3 other models gave an estimate within 10% deviation, except for the estimate for 2014 using PGH; here, this model's estimates were 17% higher compared to that of JP.

4. DISCUSSION

4.1. Model choice

P–E curves were fitted using 4 different models: JP and Webb, without a parameter for photo-inhibition and EP and PGH, with a parameter for photo-inhibition. The PGH model was unable to estimate P^{B}_{max} on 16 occasions, but in the calculations of annual production, the parameter P_s was used (Table 1); this parameter was estimated for all incubations. Different models give different estimates for photosynthetic parameters as well as estimates of production (present study), so it is important to choose one model to analyse the data. In the present study, the JP model was selected as the best model to analyse the data, however, this model lacks a photo-inhibition parameter and the carbon fixation rate was sometimes lowered at the highest irradiances (e.g. 19 June 2012; Fig. 6), suggesting the occurrence of photo-inhibition. In the present study, algal cells in small bottles were exposed to irradiances up to 1700 µmol photons m^{-2} s^{-1} for a period of 2 h. Such endured exposure to high light can result in more severe photo-inhibition compared to phytoplankton cells in the water column, where water mixing reduces the time spent in the euphotic zone (Peterson 1980, Grobbelaar 1985). The occasional depression of the carbon fixation rate at high irradiances might thus be partly the result of an incubation artefact.

How likely is a reduction of carbon fixation rates *in situ* due to exposure to excess irradiance in the western Wadden Sea? According to MacIntyre et al. (2002), photo-inhibition is most likely to occur in mixed shallow waters where the mean water column irradiance is larger than the value for E_k. At the sampling location, the average column irradiance (I_{av}, µmol photons m^{-2} s^{-1}) per day was calculated using the maximum surface irradiance during a sampling day and k_d cf. MacIntyre & Cullen (1996). Occasionally I_{av} was higher than E_k, indicating that photo-inhibition can occur. However, Grobbelaar (1985) argued that in mixed waters the severity of photo-inhibition is minimised since algal cells move rapidly in and out of the photic zone. In turbid areas, the non-photic zone might be quite large. If the mixing depth is larger than the euphotic zone, which is the case at our study location, algal cells likely spend more time in the dark. Falkowski et al. (1993) recorded mid-day depressions in photosynthetic efficiency using fast repetition rate fluorescence (frrf) measurements; the authors considered changes in the ratio of the variable fluorescence to maximum fluorescence (F_v/F_m) to be a reliable means to identify the occurrence of photo-inhibition in a system. At the Marsdiep jetty, short-term light

Table 4. Estimates of annual (g C m^{-2} yr^{-1}) and average daily (g C m^{-2} d^{-1}) production (PP) at the sampling location using curve fit parameters from the different models (see Table 1 for model specifics)

Model	2012		2013		2014	
	Annual	Daily	Annual	Daily	Annual	Daily
JP	198	0.54 ± 0.51	239	0.65 ± 1.01	131	0.36 ± 0.36
EP	203	0.56 ± 0.52	236	0.65 ± 0.96	133	0.37 ± 0.36
PGH	214	0.59 ± 0.50	244	0.67 ± 1.04	153	0.42 ± 0.43
Webb	206	0.56 ± 0.53	249	0.68 ± 1.05	138	0.38 ± 0.38

curves based on frrf measurements were applied 2014 onward, in addition to the ^{14}C incubations at the laboratory. Data from these *in situ* measurements suggest that photo-inhibition does not occur at this location (J. C. Kromkamp et al. unpubl. data). In addition, when considering the differences in annual production estimated by the 4 models, the JP model generally had the lowest annual production estimates compared to all other models (Table 4). If photo-inhibition had an effect on the production estimates, a model without photo-inhibition would overestimate production. Choosing a model without a photo-inhibition term to analyse the data thus seems legitimate here.

4.2. Photosynthetic parameters

Estimates for the photosynthetic parameters from the JP model were compared to the estimates from the other 3 models. The estimates for α^B from the other models were between 13 and 28% higher compared to the JP estimates, while for P^B_{max} the estimates were more comparable between models with only a 1–5% difference (Table 3). The difference in estimates for α^B and P^B_{max} between models as well as the higher variability in estimates for α^B have been reported before (e.g. Jassby & Platt 1976, Frenette et al. 1993, Kromkamp & Peene 1995). When comparing the JP model to the Webb model, Frenette et al. (1993) concluded that the estimates for both parameters from the Webb model were higher that the estimates made with the JP model. Kromkamp & Peene (1995) observed that the value of P^B_{max} obtained using JP was slightly smaller (<10%) than that obtained with the EP method, whereas the opposite was observed for α^B (~4% higher).

Theoretical maxima for α^B and P^B_{max} respectively have been defined as 0.11 mg C (mg chl *a*)$^{-1}$ h^{-1} (µmol photons m^{-2} s^{-1})$^{-1}$ and 25 mg C (mg chl *a*)$^{-1}$ h^{-1} (Platt & Jassby 1976, Falkowski 1981, Lohrenz et al. 1994). In the present study, estimates for α^B were higher than this maximum on 2 occasions (Day 132 in 2012 and Day 115 in 2013), and for P^B_{max} on 3 occasions (the same days as for α^B and Day 236 in 2012) (Figs. 7 & 8). Visual inspection of the curves did not reveal any abnormalities. Rates higher than the theoretical maxima have been reported in other studies as well, and in those cases were related to low chl *a* concentrations due to the dominance of small but very productive cells (Lohrenz et al. 1994, Azevedo et al. 2010). Low chl *a* concentrations could also be the result of mistakes made during filtration or incomplete extraction of pigments. In the present study, chl *a* concentrations on the dates with high values for the *P–E* parameters did not correspond to very low values of chl *a*, but the possibility that the concentrations were too low cannot be excluded. When relating environmental variables to the *P–E* parameters, the removal of outliers (see Section 2.5), which correspond to values higher than the theoretical maxima, improved the predictive model for P^B_{max} (Supplement Section 2, Table S1).

Bouman et al. (2018) reported minimum values for P^B_{max} to be 0.2 mg C (mg chl *a*)$^{-1}$ h^{-1} and 0.002 mg C (mg chl *a*)$^{-1}$ h^{-1} (µmol photons m^{-2} s^{-1})$^{-1}$ for α^B. Values for α^B and P^B_{max} lower than these rates were recorded on 19 and 22 May 2014.

Apart from the extreme values for α^B and P^B_{max}, the reported estimates for α^B and P^B_{max} in the present study were high compared to estimates reported in other studies. Within the Wadden Sea area, Tillmann et al. (2000), using the PGH model, reported that α^B varied between 0.007 and 0.039 mg C (mg chl *a*)$^{-1}$ h^{-1} (µmol photons m^{-2} s^{-1})$^{-1}$ and for P^B_{max} between 0.8 and 9.9 mg C (mg chl *a*)$^{-1}$ h^{-1} for the southern part of the German Wadden Sea in 1995–1996. In the present study, the median values for α^B and P^B_{max} in 2012 were close to the maximum values reported in Tillmann et al. (2000). The maximum value in the present study was almost twice the maximum recorded in that study. In the northern part of the German Wadden Sea in 2004, Loebl et al. (2007) reported estimates between 0.014 and 0.13 mg C (mg chl *a*)$^{-1}$ h^{-1} (µmol photons m^{-2} s^{-1})$^{-1}$ for α^B, between 1.8 and 14 mg C (mg chl *a*)$^{-1}$ h^{-1} for P^B_{max}, and between 107 and 360 µmol photons m^{-2} s^{-1} for E_k. There, the PGH model was used for curve fitting. Closer to the sampling location of the present study, Brinkman et al. (2015) reported that estimates in 2012–2013 for several locations on a transect from the Dollard towards the North Sea ranged between 0.005 and 0.25 mg C (mg chl *a*)$^{-1}$ h^{-1} (µmol photons m^{-2} s^{-1})$^{-1}$ for α^B and between 1 and 22 mg C (mg chl *a*)$^{-1}$ h^{-1} for P^B_{max}. Brinkman et al. (2015) used the EP model for curve fitting. Kamermans et al. (2014) reported that for the Marsdiep area, using PGH, α^B ranged between 0.02 and 0.12 mg C (mg chl *a*)$^{-1}$ h^{-1} (µmol photons m^{-2} s^{-1})$^{-1}$ in 2011–2013, while values for P^B_{max} were between 4 and 12 mg C (mg chl *a*)$^{-1}$ h^{-1} (values were read from the graph). Kamermans et al. (2014) also recorded photosynthetic parameter values for the same sampling location as the present study (jetty, but at low tide), with α^B ranging between 0.01 and 0.1 mg C (mg chl *a*)$^{-1}$ h^{-1} (µmol photons m^{-2} s^{-1})$^{-1}$ for 2011–2012 (April–October) and P^B_{max} between 2 and

10 mg C (mg chl *a*)$^{-1}$ h^{-1}. The estimates for α^B in the present study are comparable, while for P^B_{max} the estimates are somewhat higher. Values for E_k ranged between 60 and 540 µmol photons m^{-2} s^{-1} (Figs. 7 & 8), with minimum values at the low end of what was recorded for E_k by Kirk (1994) (between 200 and 500 µmol photons m^{-2} s^{-1}), but comparable to values reported for other locations in the Wadden Sea area (Tillmann et al. 2000, Loebl et al. 2007).

4.3. Photosynthetic parameters related to environmental variables

In the present study, the estimates for both α^B and P^B_{max} varied throughout the year. Values for α^B showed no correlation with any of the environmental variables considered, while for P^B_{max} there were significant positive correlations with SST and salinity and negative correlations with k_d, silicate and NO_{2+3} concentrations (Fig. 10). Using (a combination of) environmental variables to predict P^B_{max} resulted in a model that could explain a maximum of 30% of the variation (Supplement Section 2, Table S1). The best model, based on the lowest AIC and highest R^2, was a model that included year and SST (after removing the extreme values); none of the other environmental variables contributed significantly to the explained variance in P^B_{max} (Supplement Section 2, Table S1). Since variation in P^B_{max} due to year cannot be estimated based on remote sensing data, P^B_{max} can be described by SST, as 2.06 ± 0.67 + 0.30 ± 0.05 × SST, explaining 28% of the variation. This percentage of explained variance is equal to the 28% reported in Platt & Jassby (1976), but much lower than the 74–95% explained variance by water temperature as reported in Rae & Vincent (1998). The latter study, however, was performed under constant laboratory conditions using monocultures of phytoplankton species. Many studies have reported an exponential relationship between SST and P^B_{max} (e.g. Eppley 1972, Lohrenz et al. 1994, Tillmann et al. 2000, Macedo et al. 2001), but in the present study a linear relationship gave the best fit to the data. In 2012, values for P^B_{max} were higher than in the other 2 yr, while SST was lower compared to 2014 for most of the year (Fig. 4). The fact that SST was the variable that explained most of the variation in values of P^B_{max} does not necessarily indicate that there is a direct effect of temperature on this photosynthesis parameter, since SST correlates with other environmental variables, including nutrient concentrations (this study) and species composition (Richardson et al. 2016). However, as P^B_{max} is driven by the rate of carbon fixation, the enzymatic processes in the carbon cycle, a direct effect of temperature on P^B_{max} is to be expected and this has been demonstrated with culture studies (e.g. Morris & Kromkamp 2003).

Previous studies have found mixed results, with variations in α^B being both independent (Post et al. 1985) and dependent on water temperature (Lohrenz et al. 1994). Estimates for α^B have also been correlated with irradiance (or average of irradiance of 3 d previous) (Platt & Jassby 1976). For P^B_{max}, variation was explained by total irradiance and water temperature (Rae & Vincent 1998, Shaw & Purdie 2001) or water temperature alone (Platt & Jassby 1976, Lohrenz et al. 1994).

A strong correlation between α^B and P^B_{max} was observed. *A priori*, such a relationship is not to be expected as α^B is related to pigment composition and the chance of absorbing a photon, whereas P^B_{max} is related to processes downstream in photosystem II (PSII). Classical photo-acclimation, i.e. changing the absorption cross-section of the antenna by adding more or less photosynthetic pigments, will primarily affect α^B, but not necessarily P^B_{max}. However, many studies (e.g. Behrenfeld et al. 2004, Bouman et al. 2018 and references in both papers) observed linear relationships between α^B and P^B_{max}, as in the present study. This positive correlation has been attributed in a review by Bouman et al. (2018, p. 260) to 'a variety of physiological and ecological factors, including changes in the allocation of ATP and NADPH to carbon fixation (Behrenfeld et al., 2004), as well as changes in phytoplankton community structure (Côté and Platt, 1983)'.

From the abiotic variables that can be estimated at present from Earth Observation data, P^B_{max} can be indirectly estimated from SST (and underwater light-climate) (Behrenfeld & Falkowski 1997, Cox et al. 2010) and α^B can be derived from P^B_{max}. The low variability in α^B and P^B_{max} explained by environmental variables impedes the estimation of primary production from remotely sensed data.

E_k is generally used as an indicator of the photo-acclimation state of the phytoplankton community (Sakshaug et al. 1997). As was described by Sakshaug et al. (1997, p. 1657), 'at lower irradiances, the quantum yield of photosynthesis is higher, but the photosynthetic rate is lower; at higher irradiances, there is no major increase in the photosynthetic rate and, hence, nothing to be gained, and potentially much to be lost. Consequently, if the irradiance increases, the algae adjust their E_k upwards, and vice versa'. Based on this principle, it was expected that

variation in E_k could be related to surface irradiance (E_0), k_d or a product of both. In the present study, E_k correlated significantly with e.g. SST and k_d, but not with surface irradiance (Fig. 10). A model with k_d (with and without E_0) only explained 16% of the variation in E_k, while a model with SST explained 41% (Supplement Section 2, Table S1 & S2). The absence of a relationship between E_k and (a product of) E_0 and k_d is unexpected, and there is no satisfactory explanation for this finding.

4.4. Daily and annual primary production estimates

In the present study, no attempts were made to estimate respiratory losses in the dark. Autotrophic respiration under certain conditions might be large, resulting in negative net photic zone production. In turbid areas, Z_{eu} might be smaller than Z_{mix}, exposing the phytoplankton community to light intensities too low to support photosynthesis. To sustain positive net phytoplankton growth, the Z_{eu}:Z_{mix} ratio should be above 0.2 (e.g. Grobbelaar 1985, Cloern 1987, Alpine & Cloern 1988, Kromkamp & Peene 1995), which was the case at our sampling location, although the study by Kromkamp & Peene (1995) also obtained evidence that it might be smaller than 0.2.

Daily water column production ranged from 3.4–3800 mg C m^{-2} d^{-1}. Whether ^{14}C incubations best represent net or gross production rates is still under debate (Halsey et al. 2010, 2013, Pei & Laws 2013, Milligan et al. 2015). The rates of daily carbon fixation as well as the annual production presented in this paper are therefore referred to as 'production rates'. The seasonal pattern in daily production rates was comparable to the pattern seen in chl *a* concentrations, as has been described in other studies in the Wadden Sea (Tillmann et al. 2000). There were large differences in annual production between years, with production in 2013 being 80% higher than in 2014 (the year with the lowest annual production) and 25% higher than in 2012 (Table 4). This difference was largely due to the difference in chl *a* concentration in spring (Fig. 5). Recent findings have shown that the timing of the spring bloom is initiated by the underwater light climate, whereas the build-up of zooplankton biomass is driven by water temperature (Wiltshire & Boersma 2016). One explanation for the higher chl *a* concentration in spring in 2013 is that the low water temperature in the first half of the year (Fig. 4) suppressed zooplankton biomass, reducing grazing rates and thus allowing for a higher achieved phytoplankton biomass. In addition, the higher concentrations of silicate in 2013 compared to both other years in the pre-bloom period might have resulted in a higher phytoplankton biomass, as this might delay the onset of silicate-limitation for diatoms (Ly et al. 2014). In 2014, water temperatures were high year-round, resulting in more severe grazing, especially later in the season, explaining the low and late autumn peak in chl *a* this year (Fig. 5).

Production rates for the same location as in the present study have been published by Cadée & Hegeman (1974, 2002) and more recently by Philippart et al. (2007). Both papers present the results on carbon fixation rates using ^{14}C, but incubated samples at one fixed light intensity only. In addition, Cadée & Hegeman (1974, 2002) did not consider daily irradiances when calculating daily production rates, and assumed that light conditions were saturating during incubation. Therefore, the results from the present study will only be compared with the results published by Philippart et al. (2007). Philippart et al. (2007) followed a different procedure to calculate carbon fixation rates, which resulted in an 8% lower estimate of daily water column production compared to the present study (Supplement Section 3, Fig. S2). Annual production estimates for the period 1990–2004 were between 120 and 310 g C m^{-2} yr^{-1} and showed a steady decline over this period (Philippart et al. 2007). Annual primary production for 2012–2014 (this paper) is comparable to that of the early 2000s reported by Philippart et al. (2007). It thus seems that the decline in primary production, noted by Philippart et al. (2007) has come to a halt (or has even slightly reversed) (Fig. 12). The decline in production in the western Wadden Sea was the result of reduced riverine nutrient inputs since the mid-1980s. Since the 2000s, the decline in phosphate load has nearly come to a halt and P-concentrations are now comparable to the concentrations before the 1970s, while N-loads have been reduced to a lower extent (Cadée & Hegeman 2002, Supplement Section 4, Figs. S3 & S4).

It is generally assumed that primary production in the western Wadden Sea in spring is P-limited with likely P and silicate co-limitation for diatoms (Ly et al. 2014). Along the Dutch coast, long-term nutrient concentrations show a similar pattern as in the western Wadden Sea (Supplement Section 4, Figs. S3 & S4), suggesting that the rate of pelagic primary production might also have decreased or come to a halt here, and potentially also in other coastal seas in Europe. Additional analysis is needed to determine whether the decrease in annual primary production is confined to the western part of the Wadden Sea or if low production rates are found throughout the

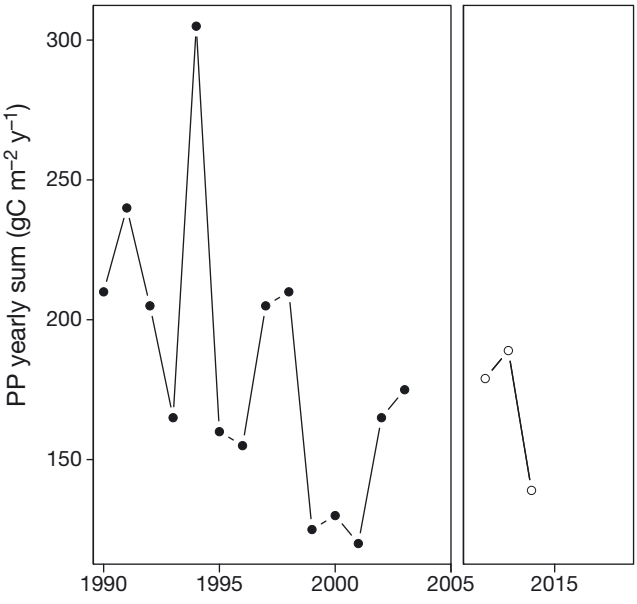

Fig. 12. The long-term trend in annual planktonic primary production (PP) at the Marsdiep jetty for the period 1990–2003 (closed circles; from Philippart et al. 2007) and for 2012, 2013 and 2014 (open circles; present study)

whole Wadden Sea. Continued monitoring of primary production is essential to find out whether the decline had halted or will continue to decline in the future.

5. CONCLUSIONS

The equation from Jassby & Platt (1976) was selected as the best model to analyse *P–E* data in the present study. This JP model lacks a parameter that allows for a reduction in the carbon fixation rate at high irradiances.

Estimates for α^B varied between 0.00024 and 0.24 mg C (mg chl *a*)$^{-1}$ h^{-1} (µmol m^{-2} s^{-1})$^{-1}$ and for P^B_{max}, between 0.1 and 48.9 mg C (mg chl *a*)$^{-1}$ h^{-1}. The estimates for α^B and P^B_{max} were correlated and showed seasonal variation, with (on average) higher values in summer and peaks in spring. There were considerable differences in values for photosynthetic parameters between years, with the highest estimates in 2012 (150% higher than in 2013, 300% higher than in 2014). The best model to estimate P^B_{max} included SST and year, but the underlying causes of this 'year-effect' remain unsolved for now. With respect to available information in space and time from Earth Observations, P^B_{max} can thus be derived from SST, explaining 28% of the variance. The absence of a correlation between α^B and environmental variables, the relatively large unresolved variance in the estimates for P^B_{max} and the large differences between years indicate that there still is some way to go before satellite measurements can be used for monitoring temporal and spatial variation in productivity.

Daily primary production varied between years with an average of 0.54 g C d^{-1} in 2012, 0.65 g C d^{-1} in 2013 and 0.36 g C d^{-1} in 2014. Annual production was calculated by linear interpolation of all parameters except irradiance, which was available for all days. The interpolated annual production for each of the 3 yr was always lowest when using the *P–E* curve fit from Jassby & Platt (1976), but differences between models were relatively small (less than 10%) between the lowest and highest estimate. Comparing the estimates for the years 2012, 2013 and 2014 with estimates published earlier indicate that the decline in planktonic primary production in the Marsdiep area since the 1990s has come to a halt. Further research will be needed to investigate the possible mechanisms underlying these changes.

Acknowledgements. The authors thank our (former) colleagues at the Royal Netherlands Institute for Sea Research: Monique Veenstra and Evaline van Weerlee for taking water samples and measurements at the jetty as well as their analysis of most environmental variables; Eric Wagemaakers for providing the data from automatic measurements at the jetty; Jan van Ooijen, Karel Bakker and Sharyn Ossebaar for nutrient analysis; Jurian Brasser for HPLC analysis; Kirsten Kooijman-Scholten and Santiago Gonzalez for 14C incubations. Jaap van der Meer is acknowledged for his constructive comments regarding the use of curve-fit models, and Gerhard Cadée for initiating the long-term time series on phytoplankton dynamics at the jetty in the early 1970s. This research was partly funded by the Dutch NWO-ZKO program IN PLACE (project no. 839.08.211). Comments by 4 anonymous reviews greatly improved the manuscript.

LITERATURE CITED

Alpine AE, Cloern JE (1988) Phytoplankton growth rates in a light-limited environment, San Francisco Bay. Mar Ecol Prog Ser 44:167–173

Arbones B, Figueiras FG, Varela R (2000) Action spectrum and maximum quantum yield of carbon fixation in natural phytoplankton populations: implications for primary production estimates in the ocean. J Mar Syst 26:97–114

Aurin DA, Dierssen HM (2012) Advantages and limitations of ocean color remote sensing in CDOM-dominated, mineral-rich coastal and estuarine waters. Remote Sens Environ 125:181–197

Azevedo IC, Duarte P, Bordalo AA (2010) Temporal and spatial variability of phytoplankton photosynthetic characteristics in a southern European estuary (Douro, Portugal). Mar Ecol Prog Ser 412:29–44

Behrenfeld MJ, Falkowski PG (1997) A consumer's guide to phytoplankton primary productivity models. Limnol Oceanogr 42:1479–1491

Behrenfeld MJ, Prasil O, Babin M, Bruyant F (2004) In search of a physiological basis for covariations in light-limited and light-saturated photosynthesis. J Phycol 40:4–25

Bouman HA, Platt T, Doblin M, Figueiras FG and others (2018) Photosynthesis–irradiance parameters of marine phytoplankton: synthesis of a global data set. Earth Syst Sci Data 10:251–266

Brinkman AG, Riegman R, Jacobs P, Kühn S, Meijboom A (2015) Ems Dollard primary production research, full data report. Report C160/14, Institute for Marine Resources and Ecosystem Studies (IMARES), Wageningen UR, Den Burg

Burnham KP, Anderson DR (2004) Multimodel inference: understanding AIC and BIC in model selection. Sociol Methods Res 33:261–304

Cadée GC, Hegeman J (1974) Primary production of the benthic microflora living on tidal flats in the Dutch Wadden Sea. Neth J Sea Res 8:240–259

Cadée GC, Hegeman J (2002) Phytoplankton in the Marsdiep at the end of the 20th century; 30 years monitoring biomass, primary production, and *Phaeocystis* blooms. J Sea Res 48:97–110

Chen J, Zhang M, Cui T, Wen Z (2013) A review of some important technical problems in respect of satellite remote sensing of chlorophyll-a concentration in coastal waters. IEEE J Sel Top Appl Earth Obs Remote Sens 6: 2275–2289

Cloern JE (1987) Turbidity as a control on phytoplankton biomass and productivity in estuaries. Cont Shelf Res 7: 1367–1381

Cloern JE (1999) The relative importance of light and nutrient limitation of phytoplankton growth: a simple index of coastal ecosystem sensitivity to nutrient enrichment. Aquat Ecol 33:3–15

Cole BE, Cloern JE (1984) Significance of biomass and light availability to phytoplankton productivity in San Francisco Bay. Mar Ecol Prog Ser 17:15–24

Cole BE, Cloern JE (1987) An empirical model for estimating phytoplankton productivity in estuaries. Mar Ecol Prog Ser 36:299–305

Côté B, Platt T (1983) Day to day variations in the spring–summer photosynthetic parameters of coastal marine phytoplankton. Limnol Oceanogr 28:320–344

Cox TJS, Soetaert K, Vanderborght JP, Kromkamp JC, Meire P (2010) Modeling photosynthesis-irradiance curves: effects of temperature, dissolved silica depletion, and changing community assemblage on community photosynthesis. Limnol Oceanogr Methods 8:424–440

Eilers PHC, Peeters JCH (1988) A model for the relationship between light intensity and the rate of photosynthesis in phytoplankton. Ecol Modell 42:199–215

Ekholm P (2008) N:P ratios in estimating nutrient limitation in aquatic systems. Finnish Environment Institute, Helsingfors

Eppley RW (1972) Temperature and phytoplankton growth in the sea. Fish Bull 70:1063–1085

Evans N, Games DE, Jackson AH, Matlin SA (1975) Applications of high-pressure liquid chromatography and field desorption mass spectrometry in studies of natural porphyrins and chlorophyll derivatives. J Chromatogr A 115:325–333

Falkowski PG (1981) Light-shade adaptation and assimilation numbers. J Plankton Res 3:203–216

Falkowski PG, Raven JA (2007) Aquatic photosynthesis. Princeton University Press, Princeton, NJ

Falkowski PG, Greene R, Kolber Z (1993) Light utilization and photoinhibition of photosynthesis in marine phytoplankton. Brookhaven National Lab, Upton, NY

Frenette JJ, Demers S, Legendre L, Dodson J (1993) Lack of agreement among models for estimating the photosynthetic parameters. Limnol Oceanogr 38:679–687

Gabarró C, Font J, Camps A, Vall llossera M, Julià A (2004) A new empirical model of sea surface microwave emissivity for salinity remote sensing. Geophys Res Lett 31: L01309

Grobbelaar JU (1985) Phytoplankton productivity in turbid waters. J Plankton Res 7:653–663

Halsey KH, Milligan AJ, Behrenfeld MJ (2010) Physiological optimization underlies growth rate-independent chlorophyll-specific gross and net primary production. Photosynth Res 103:125–137

Halsey KH, O'Malley RT, Graff JR, Milligan AJ, Behrenfeld MJ (2013) A common partitioning strategy for photosynthetic products in evolutionarily distinct phytoplankton species. New Phytol 198:1030–1038

Heip CHR, Goosen NK, Herman PMJ, Kromkamp J, Middelburg JJ, Soetaert K (1995) Production and consumption of biological particles in temperate tidal estuaries. Oceanogr Mar Biol Annu Rev 33:1–149

Herlory O, Richard P, Blanchard G (2007) Methodology of light response curves: application of chlorophyll fluorescence to microphytobenthic biofilms. Mar Biol 153: 91–101

Højerslev NK (1978) Daylight measurements appropriate for photosynthetic studies in natural sea waters. ICES J Mar Sci 38:131–146

Holmes RW (1970) The Secchi disk in turbid coastal waters. Limnol Oceanogr 15:688–694

Jamet C, Loisel H, Kuchinke CP, Ruddick K, Zibordi G, Feng H (2011) Comparison of three SeaWiFS atmospheric correction algorithms for turbid waters using AERONET-OC measurements. Remote Sens Environ 115:1955–1965

Jassby AD, Platt T (1976) Mathematical formulation of the relationship between photosynthesis and light for phytoplankton. Limnol Oceanogr 21:540–547

Joint I, Groom SB (2000) Estimation of phytoplankton production from space: current status and future potential of satellite remote sensing. J Exp Mar Biol Ecol 250: 233–255

Kamermans P, Jak R, Jacobs P, Riegman R (2014) Groei en begrazing van mosselzaad, primaire productie en picoplankton in de Waddenzee Technisch Rapport project. Meerjarige effect- en productiemetingen aan MZI's in de Westelijke Waddenzee, Oosterschelde en Voordelta. Report no. C187/13, IMARES Wageningen UR, Yerseke

Kirk JTO (1994) Light and photosynthesis in aquatic ecosystems. Cambridge University Press, Cambridge

Klemas V (2011) Remote sensing of sea surface salinity: an overview with case studies. J Coast Res 27:830–838

Kromkamp J, Peene J (1995) Possibility of net phytoplankton primary production in the turbid Schelde Estuary (SW Netherlands). Mar Ecol Prog Ser 121:249–259

Lee Z, Shang S, Du K, Wei J (2018) Resolving the long standing puzzles about the observed Secchi depth relationships. Limnol Oceanogr 63:2321–2336

Lewis MR, Smith JC (1983) A small volume, short-incubation-time method for measurement of photosynthesis as a

function of incident irradiance. Mar Ecol Prog Ser 13: 99–102
Loebl M, Dolch T, van Beusekom JE (2007) Annual dynamics of pelagic primary production and respiration in a shallow coastal basin. J Sea Res 58:269–282
Lohrenz SE, Fahnenstiel GL, Redalje DG (1994) Spatial and temporal variations of photosynthetic parameters in relation to environmental conditions in coastal waters of the northern Gulf of Mexico. Estuaries 17:779–795
Longhurst A, Sathyendranath S, Platt T, Caverhill C (1995) An estimate of global primary production in the ocean from satellite radiometer data. J Plankton Res 17: 1245–1271
Ly J, Philippart CJM, Kromkamp JC (2014) Phosphorus limitation during a phytoplankton spring bloom in the western Dutch Wadden Sea. J Sea Res 88:109–120
Macedo MF, Ferreira JG, Duarte P (1998) Dynamic behaviour of photosynthesis-irradiance curves determined from oxygen production during variable incubation periods. Mar Ecol Prog Ser 165:31–43
Macedo MF, Duarte P, Mendes P, Ferreira JG (2001) Annual variation of environmental variables, phytoplankton species composition and photosynthetic parameters in a coastal lagoon. J Plankton Res 23:719–732
MacIntyre HL, Cullen JJ (1996) Primary production by suspended and benthic microalgae in a turbid estuary: timescales of variability in San Antonio Bay, Texas. Mar Ecol Prog Ser 145:245–268
MacIntyre HL, Kana TM, Anning T, Geider RJ (2002) Photoacclimation of photosynthesis irradiance response curves and photosynthetic pigments in microalgae and cyanobacteria. J Phycol 38:17–38
Milligan AJ, Halsey KH, Behrenfeld MJ (2015) Advancing interpretations of ^{14}C-uptake measurements in the context of phytoplankton physiology and ecology. J Plankton Res 37:692–698
Morris EP, Kromkamp JC (2003) Influence of temperature on the relationship between oxygen- and fluorescence-based estimates of photosynthetic parameters in a marine benthic diatom (*Cylindrotheca closterium*). Eur J Phycol 38:133–142
Muller-Karger FE, Miloslavich P, Bax NJ, Simmons S and others (2018) Advancing marine biological observations and data requirements of the complementary essential ocean variables (EOVs) and essential biodiversity variables (EBVs) frameworks. Front Mar Sci 5:211
Nauw JJ, Merckelbach LM, Ridderinkhof H, Van Aken HM (2014) Long-term ferry-based observations of the suspended sediment fluxes through the Marsdiep inlet using acoustic Doppler current profilers. J Sea Res 87: 17–29
Pei S, Laws EA (2013) Does the ^{14}C method estimate net photosynthesis? Implications from batch and continuous culture studies of marine phytoplankton. Deep Sea Res I 82:1–9
Pennock JR, Sharp JH (1994) Temporal alternation between light- and nutrient-limitation of phytoplankton production in a coastal plain estuary. Mar Ecol Prog Ser 111: 275–288
Pereira HM, Ferrier S, Walters M, Geller GN and others (2013) Essential biodiversity variables. Science 339: 277–278
Peterson BJ (1980) Aquatic primary productivity and the ^{14}C-CO_2 method: a history of the productivity problem. Annu Rev Ecol Syst 11:359–385
Philippart CJ, Cadée GC, van Raaphorst W, Riegman R (2000) Long term phytoplankton nutrient interactions in a shallow coastal sea: algal community structure, nutrient budgets, and denitrification potential. Limnol Oceanogr 45:131–144
Philippart CJM, Beukema JJ, Cadée GC, Dekker R and others (2007) Impacts of nutrient reduction on coastal communities. Ecosystems 10:96–119
Platt T, Jassby AD (1976) The relationship between photosynthesis and light for natural assemblages of coastal marine phytoplankton. J Phycol 12:421–430
Platt T, Gallegos CL, Harrison WG (1980) Photoinhibition and photosynthesis in natural assemblages of marine phytoplankton. J Mar Res 38:687–701
Post AF, Dubinsky Z, Wyman K, Falkowski PG (1985) Physiological responses of a marine planktonic diatom to transitions in growth irradiance. Mar Ecol Prog Ser 25: 141–149
R Core Team (2018) R: a language and environment for statistical computing. R Foundation for Statistical Computing, Vienna
Rae R, Vincent WF (1998) Phytoplankton production in subarctic lake and river ecosystems: development of a photosynthesis-temperature-irradiance model. J Plankton Res 20:1293–1312
Redfield AC (1958) The biological control of chemical factors in the environment. Am Sci 46:205–221
Richardson K, Bendtsen J, Kragh T, Mousing EA (2016) Constraining the distribution of photosynthetic parameters in the Global Ocean. Front Mar Sci 3:269
Ridderinkhof H (1988) Tidal and residual flows in the western Dutch Wadden Sea II: an analytical model to study the constant flow between connected tidal basins. Neth J Sea Res 22:185–198
Sakshaug E, Bricaud A, Dandonneau Y, Falkowski PG and others (1997) Parameters of photosynthesis: definitions, theory and interpretation of results. J Plankton Res 19: 1637–1670
Shaw PJ, Purdie DA (2001) Phytoplankton photosynthesis-irradiance parameters in the near-shore UK coastal waters of the North Sea: temporal variation and environmental control. Mar Ecol Prog Ser 216:83–94
Silsbe GM, Malkin SY (2015) phytotools: phytoplankton production tools. R package version 1.0. https://CRAN.R-project.org/package=phytotools
Spiess AN, Neumeyer N (2010) An evaluation of R^2 as an inadequate measure for nonlinear models in pharmacological and biochemical research: a Monte Carlo approach. BMC Pharmacol 10:6
Strickland JD, Parsons TR (1972) A practical handbook of seawater analysis. Bull Fish Res Board Can 167:1–310
Talling JF (1957) Photosynthetic characteristics of some freshwater plankton diatoms in relation to underwater radiation. New Phytol 56:29–50
Tillmann U, Hesse KJ, Colijn F (2000) Planktonic primary production in the German Wadden Sea. J Plankton Res 22:1253–1276
Webb WL, Newton M, Starr D (1974) Carbon dioxide exchange of *Alnus rubra*: a mathematical model. Oecologia 17:281–291
Wiltshire KH, Boersma M (2016) Meeting in the middle: on the interactions between microalgae and their predators or zooplankton and their food. In: Glibert PM, Kana TM (eds) Aquatic microbial ecology and biogeochemistry: a dual perspective. Springer, Cham, p 215–223

Editorial responsibility: Katherine Richardson, Copenhagen, Denmark

Submitted: September 11, 2019; Accepted: February 17, 2020
Proofs received from author(s): March 28, 2020